

Article

The Impact of Biofilms upon Surfaces Relevant to an Intermediate Level Radioactive Waste Geological Disposal Facility under Simulated Near-Field Conditions

Christopher J. Charles ¹, Simon P. Rout ¹, Andrew P. Laws ², Brian R. Jackson ³, Sally A. Boxall ³ and Paul N. Humphreys ^{1,*} 

¹ Department of Biological Sciences, School of Applied Sciences, University of Huddersfield, Queensgate, Huddersfield HD1 3DH, UK; christopher.charles@hud.ac.uk (C.J.C.); s.rout@hud.ac.uk (S.P.R.)

² Department of Chemical Sciences, School of Applied Sciences, University of Huddersfield, Queensgate, Huddersfield HD1 3DH, UK; a.p.laws@hud.ac.uk

³ Bio-Imaging Facility, School of Molecular and Cellular Biology, Faculty of Biological Sciences, University of Leeds, Leeds LS2 9JT, UK; b.r.jackson@leeds.ac.uk (B.R.J.); s.a.boxall@leeds.ac.uk (S.A.B.)

* Correspondence: p.n.humphreys@hud.ac.uk; Tel.: +44-1484-472771

Received: 27 April 2017; Accepted: 7 July 2017; Published: 12 July 2017

Abstract: The ability of biofilms to form on a range of materials (cementitious backfill (Nirex Reference Vault Backfill (NRVB)), graphite, and stainless steel) relevant to potential UK intermediate level radioactive waste (ILW) disposal concepts was investigated by exposing these surfaces to alkaliphilic flocs generated by mature biofilm communities. Flocs are aggregates of biofilm material that are able to act as a transport vector for the propagation of biofilms. In systems where biofilm formation was observed there was also a decrease in the sorption of isosaccharinic acids to the NRVB. The biofilms were composed of cells, extracellular DNA (eDNA), proteins, and lipids with a smaller polysaccharide fraction, which was biased towards mannopyranosyl linked carbohydrates. The same trend was seen with the graphite and stainless steel surfaces at these pH values, but in this case the biofilms associated with the stainless steel surfaces had a distinct eDNA basal layer that anchored the biofilm to the surface. At pH 13, no structured biofilm was observed, rather all the surfaces accumulated an indistinct organic layer composed of biofilm materials. This was particularly the case for the stainless steel coupons which accumulated relatively large quantities of eDNA. The results demonstrate that there is the potential for biofilm formation in an ILW-GDF provided an initiation source for the microbial biofilm is present. They also suggest that even when conditions are too harsh for biofilm formation, exposed surfaces may accumulate organic material such as eDNA.

Keywords: NRVB; intermediate level waste; alkaliphilic; biofilm; engineered barrier; graphite; stainless steel; carbonation; isosaccharinic acid; eDNA

1. Introduction

One of the current proposed strategies for the disposal of intermediate level radioactive wastes (ILW) in the UK is that of a cementitious, geological disposal facility (GDF) [1]. A GDF operates using a multi-barrier system of natural and engineered materials which act to retain the waste and to retard the migration of radionuclides out of the facility and into the biosphere [2]. The first such barrier arises from the physical packaging of conditioned waste into steel or concrete containers [3]. These waste packages are then placed within a subterranean vault and subsequently surrounded with a cement based backfill forming the second barrier; one possible backfill is the NRVB for use in a higher strength host rock [2,4]. After closure of the GDF, groundwater resaturation results in an alkaline porewater

through conditioning by the backfill that contributes to the chemical containment of radionuclides via their precipitation and sorption (the backfill sorbs radionuclides from solution) [2]. A third barrier is that of the host rock whereby the local geochemical conditions act to immobilize radionuclides by sorption onto the host rock surface [5].

ILW contains a range of cellulose bearing materials which are expected to undergo chemical hydrolysis under the chemically reducing, alkaline conditions (~pH 12.5) expected to develop within the near field of the GDF [6,7]. The major components of these cellulose degradation products (CDP) are the alpha and beta diastereomers of isosaccharinic acid (ISA) (alpha = ((2S,4S)-2,4,5-trihydroxy-2-(hydroxymethyl)pentanoic acid; beta = (2R,4S)-2,4,5-trihydroxy-2-(hydroxymethyl)pentanoic acid), which have been shown to affect the solubility of radionuclides under near field conditions through the formation of complexes [6]. Cement has been shown to sorb the alpha form of ISA, however, there are no data available for the beta form [8], the sorption of ISA to cement reduces the amount of ISA available to influence radionuclide sorption [8].

It is anticipated that microbes will be present within an ILW-GDF, but will require reduced pH microsites in order to proliferate [9]. Microbes which can survive under these harsh conditions and utilize ISA and other cellulose degradation products as a carbon source could affect the long term performance of such a facility. This could be through the metabolism of complexants [10,11], the modification of surface properties through the generation of biofilms [12], the catalysis of redox reactions and the carbonation of the cementitious materials [13]. Recent studies on industrial alkaline sites have shown that diverse microbial communities can exist at in situ pH values up to pH 12 [10,11]. Microcosm experiments using sediments and biofilms generated in situ from this site have shown the ability of the local consortia to degrade both forms of ISA up to pH 11 [14,15]. Further work has shown the ability of floc based communities derived from these sediments to be capable of short term survival (weeks) at pH 13 by the generation of lower pH microsites within the interior of these flocs [16]. These floc based communities have the potential, depending on the local physical environment, to act as a transport vector, allowing the microbial colonisation of an ILW-GDF from both external sources and from biofilms formed within the near field [16].

Within the present study, the ability of these flocs to act as a transport vector for microorganisms and to establish biofilm communities on NRVB and other surfaces relevant to an ILW-GDF (304L stainless steel, 316L stainless steel, and graphite) was investigated within a laboratory flow cell. These NRVB flow cells and the associated coupons were exposed to multispecies flocs generated by mature CDP metabolizing biofilms. The generated data provide an insight into the ability of microbial communities to form and propagate within a cementitious ILW-GDF through the formation of biofilms on the exposed surfaces, e.g., within cracks in the engineering materials likely to be present.

2. Materials and Methods

Nirex reference vault backfill (NRVB) was prepared using methods outlined by Butcher et al. [4] with the final composition shown in Table 1. NRVB was cast into biocell units (Figure S1) to give an approximate final dried weight of 103 g per biocell. 2 × grade 304L austenitic stainless steel discs, 2 × grade 316L austenitic stainless steel discs (2 cm diameter, 1.2 mm thickness, 2B Mill finish) (Syspal, Telford, UK) and a ~1 cm diameter graphite disc were then placed into the NRVB. After casting, the NRVB was allowed to harden overnight and then cured in a sealed biocell for 28 days under saturated Ca(OH)₂ solution at room temperature. Once constructed, the biocell had an ≈ 1 mm gap between the NRVB surface and the top of the flow cell through which the reaction liquid flowed.

Table 1. NRVB composition.

Component	Mass (g)
Lime	300
Limestone flour	990
Portland cement	900
Water	1230

The floc forming community described in Charles et al. [14,16] was employed as a seed culture for these experiments. The seed culture (50 mL) was prepared in a pH 11 system (500 mL microcosm) fed 10% v/v CDP solution [17] diluted in mineral media [18] giving a concentration of 5 mM ISA. This seed culture was then recirculated at rate of 0.05 mL min⁻¹ through sand-filled biocell units for 10 weeks to establish a biofilm for propagation. This approach was employed because it generated a consistent source of flocs. Once established, the sand biofilms were then connected in series to the NRVB biocells in a single pass configuration with a feed and collection vessel attached (Figure 1 and Figure S2). Sample ports at the inflow and outflow of the NRVB column allowed liquid samples to be removed every two days. The flow rate of the system was set to deliver 1 L of 10% CDP in mineral media at pH 11, 12, or 13 over a 14 day period. The concentration of ISA within all samples was determined using HPAEC-PAD as previously described by Rout et al. [17] and pH determined using a probe and handheld unit (Mettler Toledo, Leicester, UK). Controls were run in duplicate using the same system and sampling period using a sterile sand column in place of a biofilm. All systems were run under anoxic conditions.

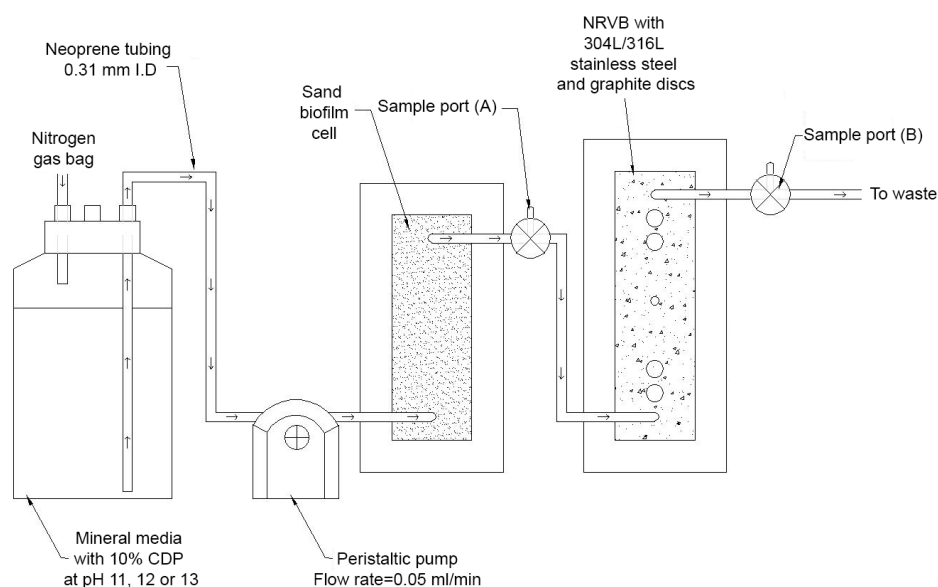


Figure 1. Biocell configuration. The single pass system outlined above was used to determine the impact of biofilms under ILW-GDF conditions upon associated repository materials.

After 14 days, the surface of the NRVB was tested for evidence of carbonation by using 1% (w/v) phenolphthalein ethanol solution [19]. The solution was added directly onto the NRVB surface with alkaline areas showing a purple/red colour and fully carbonated areas becoming colourless. Samples for microscopy analysis were initially fixed in 4% paraformaldehyde made up in phosphate buffered saline (PBS) overnight at 4 °C and then washed twice with PBS. Samples were then placed into a storage ethanol-TRIS storage buffer described by Charles et al. [14] and stored at −20 °C prior to analysis.

The surfaces of the NRVB, steel, and graphite exposed to biotic conditions were investigated at all pH values via confocal laser scanning microscopy (CLSM) at the Bio Imaging Centre of Leeds University using a Zeiss LSM880 inverted confocal microscope with image analysis performed using

Zen 2.1 (Zeiss Microscopy, Oberkochen, Germany). A five-colour staining method to visualize different extracellular polymeric substances (EPS) components was undertaken in accordance with the methods outlined by Chen et al. [20]. Briefly: Calcofluor white was used for the visualisation of β -1,4 and β -1,3 polysaccharides (Sigma-Aldrich, Gillingham, UK), Nile red (Fisher Scientific, Loughborough, UK) for lipids and hydrophobic sites, Concanavalin A, Tetramethylrhodamine Conjugate (Fisher Scientific) for α -Mannopyranosyl, α -glucopyranosyl sugars, FITc (Fisher Scientific) for protein and Syto 63 (Fisher Scientific) for total cells and extracellular DNA. Unstained samples were used as autofluorescence controls.

All surfaces exposed to biotic and abiotic control conditions at all pH values were investigated using a Quanta FEG 250 scanning electron microscope (SEM) and energy-dispersive X-ray spectroscopy (EDS) to compare surface morphology and elemental composition. Fixed samples (described previously) were dehydrated using a serial ethanol dilution of 25, 50, 75, and 100% for 2 min per step. Samples were then dried and sputter coated via a gold palladium plasma (CA7625 Polaron, Quorum Technologies Ltd, Laughton, UK).

To determine the microbial load present in the effluent leaving the NRVB biocell liquid was collected from sample port B (Figure 1), stained using a Live/Dead BacLite™ kit (Thermo-Fisher, Runcorn, UK) and visualised using an Olympus BX41 microscope (Olympus, Southend-on-Sea, UK). ATP content at the NRVB outlet was determined using a 3M Clean-Trace Biomass Detection Kit and Luminometer (3M, Bracknell, UK) employing a modified method described previously by Charles et al. [14] with cell density calculated against a standard curve of *E. coli* K12 cells.

3. Results and Discussion

The sand biofilms generated multispecies flocs as previously observed [14,16] (Figure 2), some of which were able to survive transit across the NRVB surface at all influent pH values. However, the majority of the flocs entering the biocells were retained on the NRVB surface (>99% on a dry weight basis). This retention reduced the microbial load from an average influent level of between 10^4 and 10^5 cfu/mL to approximately 10^2 cfu/mL.

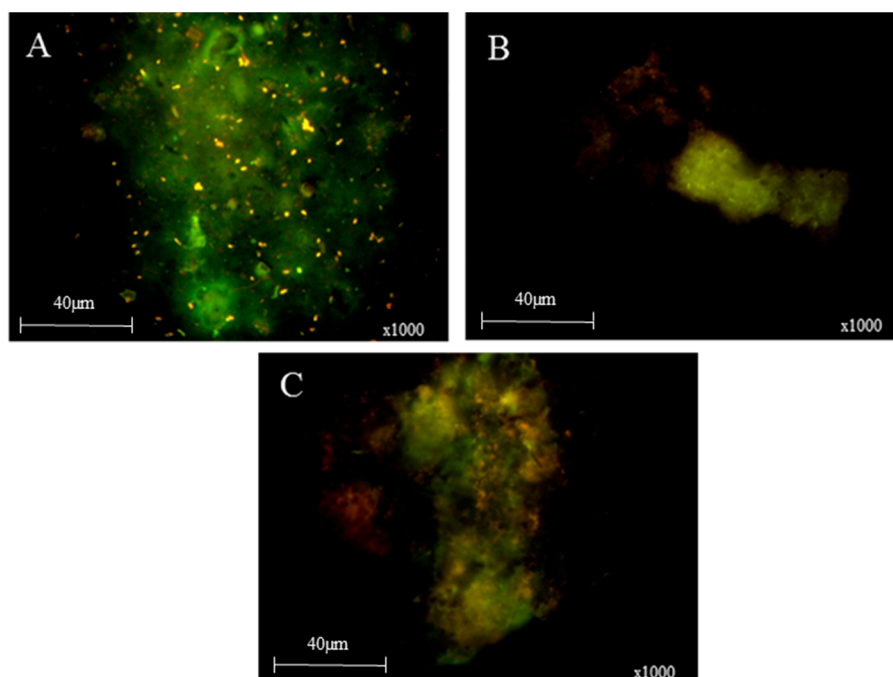


Figure 2. Multispecies flocs survived transit across the NRVB surface. Live/dead staining of the microbial flocs leaving the NRVB columns at (A) pH 11, (B) pH 12, and (C) pH 13 indicated that the flocs were able to survive transit across the surface of the NRVB.

Irrespective of the influent pH values, interaction with the NRVB columns increased the initial effluent pH values (before biofilm formation) to above pH 13, an observation consistent with previous NRVB studies [4]. The only exception being the column receiving the pH 11 influent where the initial effluent pH ranged from a maximum of pH 13.1 to a minimum of pH 12.6. Biofilm development on the NRVB surfaces was dependent on the influent pH. In the case of the pH 11 influent, biofilm established within crevices in the NRVB and was predominantly composed of extracellular DNA (eDNA), cells, proteins, and lipids with a smaller polysaccharide fraction which was biased towards mannopyranosyl-linked carbohydrates (Figure 3). The level of surface colonisation decreased when the influent pH was increased to pH 12.0 with small patches of biofilm visible that were again rich in eDNA, lipids, and mannopyranosyl linked carbohydrates. At pH 13.0 no biofilm was formed, rather the flocs were lysed and their organic components were evenly spread over the NRVB surface reflecting the grout's ability to sorb organic material. A similar observation was made by Grant et al. [21] whilst working on ISA degrading denitrifying systems, they observed that biofilm formation followed the creation of a thin organic priming layer [22] on the NRVB surface which was associated with surface carbonation [21].

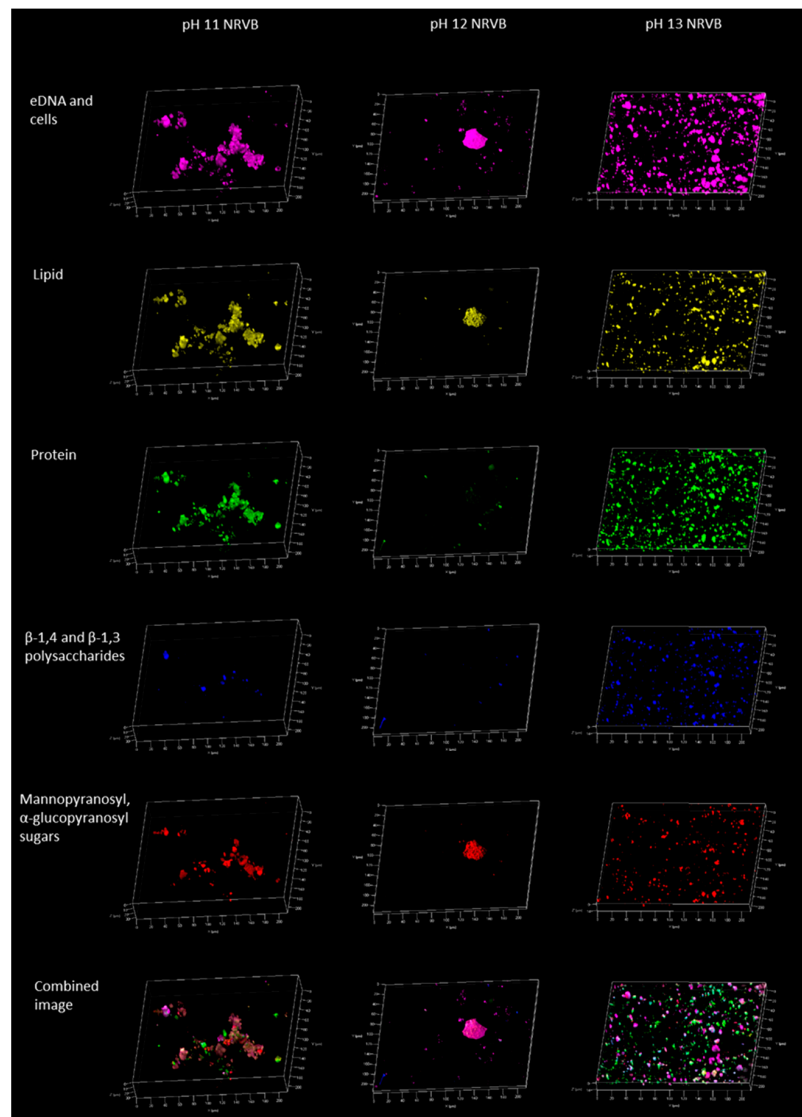


Figure 3. Five colour CLSM imaging of biofilm components on NRVB. At influent pH values of pH 11 and 12, biofilms formed within crevices with a reduced colonisation at pH 12. At pH 13, no obvious biofilm could be observed, however floc organic components were evenly spread across the NRVB surface.

Surface pH reduction was evident in all the biotic systems following phenolphthalein staining (Figure S3A) most likely associated with surface carbonation. Within biotic samples, the surfaces showed areas of increased surface roughness associated with areas of EPS materials. Carbonation and calcite formation are commonly associated with microbial activity under alkaline conditions [23] with the associated biofilms generating EPS that promote biofilm adherence to calcite surfaces [24]. In this case carbonation is likely to be due to both inorganic carbon entering the NRVB biocell from the sand biofilm and that generated by microbial activity on the NRVB column at pH 11 and 12 (Figure S3B). The carbonation of NRVB has a number of potential impacts on repository performance including retarding the migration of radioactive carbon dioxide through precipitation reactions [25], carbonation has also been shown to seal cracks and pores, which may retard radionuclide migration by reducing permeability [26]. A reduction in permeability may decrease the ability of a gas phase, which could be formed from the degradation of organic matter and corrosion of metals, to move through the engineered barrier system of the GDF [26].

Comparison of influent and effluent leachates indicated that the removal of all forms of ISA occurred in both biotic and abiotic NRVB biocells (Figure 4), reflecting the ability of NRVB to sorb these compounds. With the exception of the pH 13 system, the removal of ISA from biotic systems was less than that observed in the abiotic systems indicating that microbiological activity was attenuating the ability of the NRVB to sorb ISA via a combination of biofilm formation and surface carbonation. The anaerobic degradation of ISA under alkaline conditions has previously been shown to be via a fermentation pathway to acetate, CO₂, and hydrogen [14], resulting in acidification of the local environment [10]. The fermentation of ISA in the NRVB flow cells receiving pH 11 and 12 influents, resulted in a reduction in pH (Figure S4) and formation of carbonates as indicated by an increase in inorganic carbon (Figure S5). Within abiotic cells, it is likely that the pH increases observed are likely due to interactions with the NRVB, allowing for the dissolution of hydroxides. At pH 13, no detectable changes in pH were observed and the removal of the three forms of ISA was, if anything, slightly greater than in the abiotic system. Cement has previously been shown to bind alpha ISA [8], in addition to alpha ISA, the abiotic NRVB systems were also able to bind beta ISA and xylo ISA (a hemicellulose degradation product [27]). As the influent pH increased from pH 11 to pH 12 the amount of all forms of ISA bound to the abiotic NRVB columns increased, whilst sorption in the pH 12 and pH 13 experiments were similar (Figure 4). The reduction in ISA removal seen in these two biotic systems when compared to the abiotic controls indicates that biofilm formation and microbial activity has reduced the ability of the NRVB surface to retain ISA by the blinding of the sorption sites. These observations suggest that biofilm formation may affect the concentration of ISA in the near field of a GDF due to a reduction in the ability of NRVB to interact with ISA. Other authors have noted the ability of microbial activity to degrade ISA at high pH; a competing effect [28].

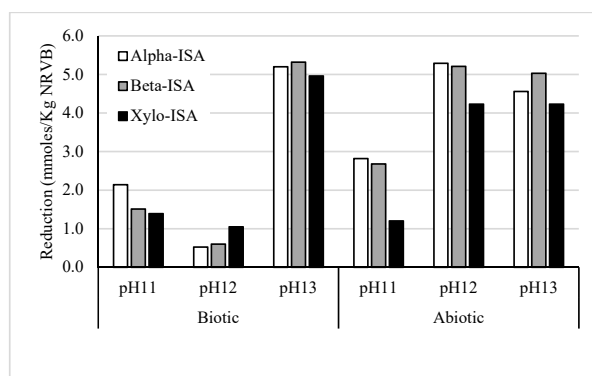


Figure 4. Isosaccharinic acid removal. The removal of isosaccharinic acids in both the biotic and abiotic experiments indicated that both sorption and microbial degradation was occurring, the latter is highlighted by the reduction in pH of the liquid leaving the biotic experiments (Figure S4).

In the case of the embedded materials (graphite and steel) biofilm development in the biotic systems followed a similar pattern to that seen on the NRVB. At an influent pH of pH 11, there were clear coverings of cells and EPS interspersed with more crystalline regions coating the surfaces of each material. As the influent pH increased to pH 12, the amount of surface coverage by cells and EPS was reduced. CLSM imaging of the graphite and stainless steel associated biofilms showed two distinct structures across these two surface types (Figure 5A–C). The graphite associated biofilms were generally thicker (~16 μm) than those found on the surface of both the 304 and 316 stainless steels (~8 μm). Structurally, the graphite biofilm had a thick, multicomponent basal layer (Figure 5A) at the graphite surface with a lipid and polysaccharide dominated mid and upper layer. In contrast, the biofilms formed on both stainless steel types were anchored to the surface by 3–4 μm layer of eDNA (Figure 5B,C) with a distinct lipid and polysaccharide rich mid and upper layer. As the influent pH increased to pH 13, the graphite and steel surfaces accumulated organic material, with both grades of stainless steel accumulating comparatively large stacks (18–30 μm) of eDNA. Although at pH 13 no structured biofilm could be distinguished, the accumulation of eDNA at the steel surface could be a precursor to biofilm formation if the ambient pH was to be attenuated later by microbial activity. This is supported by the fact that the biofilms which formed on the surface of the stainless steels at lower influent pH values (e.g., pH 12) had a clear eDNA basal layer upon which the rest of the biofilm was built.

Although originally reported with respect to clinical research themes, a number of studies have demonstrated the importance of eDNA in biofilm formation [28,29]. In environmental isolates, eDNA has been shown to have a role in the initiation of biofilm development [30] and the promotion of floc formation in marine [31] and alkaliphilic microorganisms [16]. The anionic nature of eDNA results in strong interactions between eDNA and metal cations such as Ca^{2+} ions, such interactions between eDNA and Ca^{2+} ions have been shown to promote aggregation and biofilm formation [32]. In the experiments reported here the precipitation of calcium carbonate onto the steel surface may be promoting the accumulation of eDNA. However, this does not explain the differences between the organic layers formed on the graphite coupons which were more organically diverse when compared to the eDNA dominated layers seen on the stainless steel. This suggests a direct interaction between the eDNA and the steel at alkaline pH is promoting this accumulation at these elevated pHs. There is little published data on interactions between eDNA and steel surfaces and what is available has focused on bacteria such as *Campylobacter* under aerobic conditions [33] giving it limited relevance to an ILW-GDF. However, the data gathered here suggests that eDNA originating from microbial cells will modify steel surfaces at alkaline pH provided sufficient microbial biomass is present.

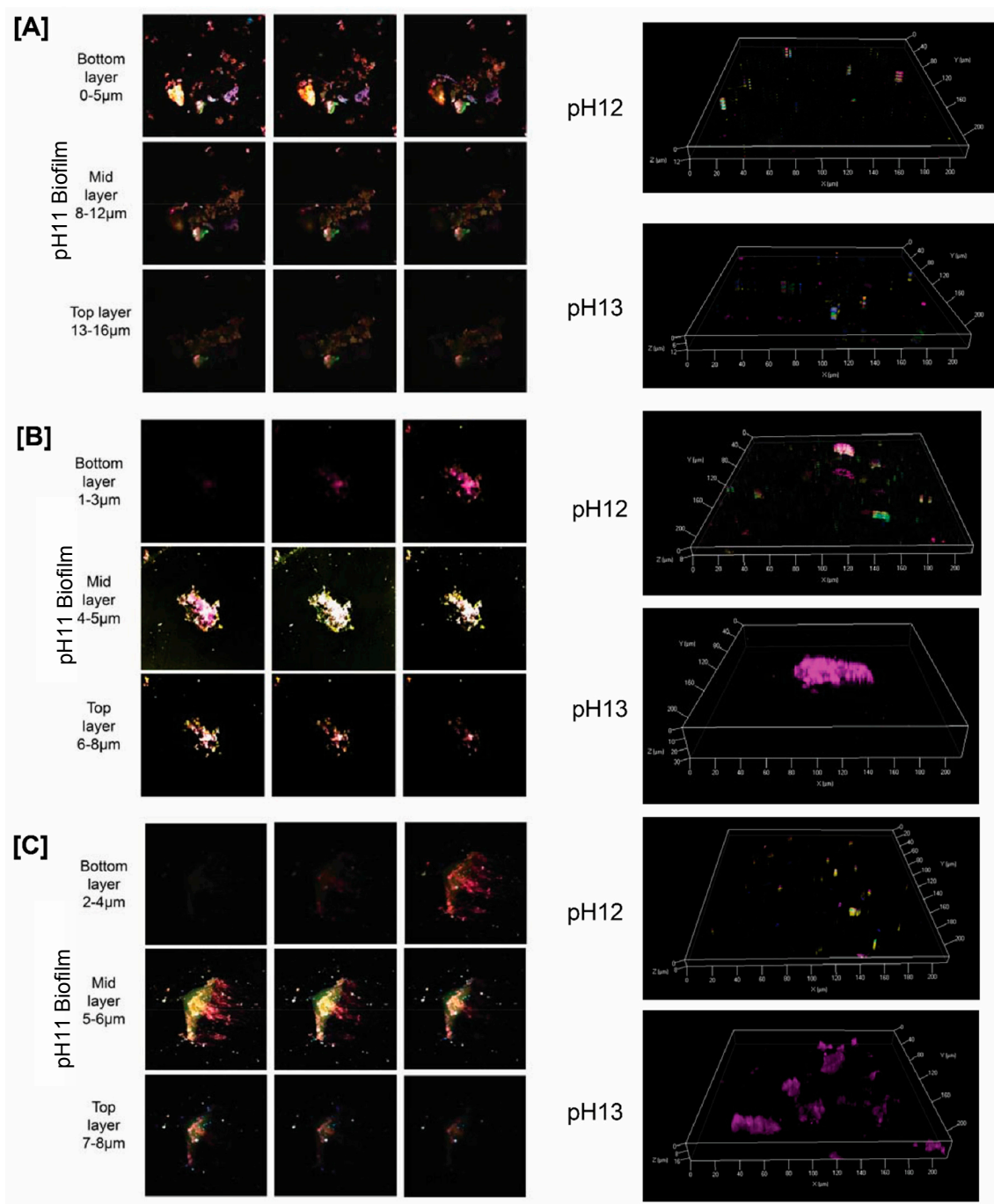


Figure 5. CLSM imaging of surface associated EPS components. (A) 16 µm thick biofilm grew on the surface of graphite (A) at pH 11, with an even dispersal of organic components sorbing to the surface at pH 12 and 13. eDNA composed a basal layer of biofilm at pH 11 on the surface of both 304L (B) and 316L (C) stainless steel surfaces and could be seen to have an affinity to the surface at pH 13 despite no obvious biofilm.

4. Conclusions

This investigation demonstrates that the sloughing of biofilms and the associated release of flocs is a potential transport mechanism for microbes within an ILW-GDF. The successful colonisation of graphite, stainless steel, and NRVB surfaces within a relatively short period of time indicates that when growing as a biofilm, alkaliphilic microbial communities can survive on ILW-GDF relevant

surfaces. The structure of the biofilms formed was surface dependent with the NRVB and graphite biofilms having a complex eDNA, lipid, and polysaccharide structure. The steel on the other hand had a clear eDNA base which anchored the more complex biofilm to the steel surface. The formation of these biofilms was only possible however, when the ambient pH was below pH 13. This indicates that in order to propagate through cracks or fissures in the NRVB, microbes would require an initiation point of active microbial metabolism. Such an initiation point could for example be associated with an actively growing biofilm or a region of cellulosic waste that has acidified due to microbial activity [10]. In the presence of an active biofilm, the sorption of ISA to the NRVB was reduced by limiting the interaction of the NRVB with the solution. Thus, one impact of microbial activity could be increased transport of complexants such as ISA through the near field. However, it should be noted that in an actual ILW-GDF a wide range of other factors will contribute to the overall transport of complexants, including microbial degradation of complexants, consequently at this stage the impact of these microbial process on facility performance is not quantifiable. At the highest pH values where no biofilm was established, all the test surfaces (NRVB, graphite, and steel) became conditioned by the organic components of the microbial flocs, indicating that isolated areas of microbial activity may have wider impacts on the surfaces present within an ILW-GDF. The binding of these organic components may act as a point of attachment for the generation of new biofilms if the overall pH were to fall far enough. This is best illustrated by the steel samples where eDNA was preferentially accumulated on the steel surface and eDNA was seen to anchor the biofilms that formed on these surfaces. Overall, the study demonstrates that the formation of biofilms in the highly alkaline near field of a proposed ILW-GDF is possible provided an initiation point of below pH 12.0 is present. These biofilms will have direct and indirect impacts on the performance of these surfaces through both carbonation and the accumulation of organic biofilm components. These observations emphasize the importance of heterogeneity within the near-field since any areas of reduced pH could allow the initiation of an active microbial population that could then propagate throughout the facility.

Supplementary Materials: The following are available online at www.mdpi.com/2076-3263/7/3/57/s1, Figure S1: Diagram of large biocell unit used to house NRVB column. Figure S2: Reaction set up. Biofilm was established on the sand column by recirculation of a flocculate forming seed culture for 10 weeks. The sand column was then challenged with 10% mineral media at pH 11 and flowed through into the NRVB column (B). The sand was then replaced with fresh sand and the process of establishment of biofilm at pH 11 repeated, before being challenged with 10% CDP and mineral media at pH 12 and 13. Figure S3: Carbonation of NRVB surfaces. Carbonation (white areas) was observed in all biotic samples following phenolphthalein staining (A), where SEM imaging (B) indicated modifications to the NRVB surfaces at influent pH values of pH 11, 12, and 13. Figure S4: pH evolution at outlet of NRVB column. Figure S5: Accumulation of dissolved inorganic carbon at outlet port.

Acknowledgments: The Zeiss LSM880 microscope was purchased with a Wellcome Trust multi-user equipment award: WT104918MA. The experimental work reported here was partially funded by Radioactive Waste Management Limited.

Author Contributions: Christopher J. Charles, Simon P. Rout, Andrew P. Laws, and Paul N. Humphreys conceived and designed the experiments. Christopher J. Charles performed the experiments and analysed the data. Christopher J. Charles, Simon P. Rout, and Paul N. Humphreys contributed to manuscript preparation. Brian R. Jackson and Sally A. Boxall assisted with CLSM investigation.

Conflicts of Interest: The authors declare no conflict of interest.

References

1. N.D.A. *Geological Disposal: An Introduction to the Generic Disposal System Safety Case*; NDA/RWMD/010; Nuclear Decommissioning Authority (Radioactive Waste Management Directorate): Didcot, UK, 2010.
2. N.D.A. *Geological Disposal: Near-Field Evolution Status Report*; NDA/RWMD/033; Nuclear Decommissioning Agency (Radioactive Waste Management Directorate): Didcot, UK, 2010.
3. N.D.A. *Geological Disposal: Package Evolution Status Report*; NDA/RWMD/031; Nuclear Decommissioning Authority (Radioactive Waste Management Directorate): Didcot, UK, 2010.
4. Butcher, E.J.; Borwick, J.; Collier, N.; Williams, S.J. Long term leachate evolution during flow-through leaching of a vault backfill (NRVB). *Mineral. Mag.* **2012**, *76*, 3023–3031. [[CrossRef](#)]

5. N.D.A. *Geological Disposal: Geosphere Status Report*; NDA/RWMD/035; Nuclear Decommissioning Authority (Radioactive Waste Management Directorate): Didcot, UK, 2010.
6. Humphreys, P.; Laws, A.; Dawson, J. *A Review of Cellulose Degradation and the Fate of Degradation Products under Repository Conditions*; SERCO/TAS/002274/001 Serco Contractors Report for the Nuclear Decommissioning Authority; Serco: Didcot, UK, 2010.
7. Knill, C.J.; Kennedy, J.F. Degradation of cellulose under alkaline conditions. *Carbohydr. Polym.* **2003**, *51*, 281–300. [[CrossRef](#)]
8. Van Loon, L.R.; Glaus, M.A.; Stallone, S.; Laube, A. Sorption of isosaccharinic acid, a cellulose degradation product, on cement. *Environ. Sci. Technol.* **1997**, *31*, 1243–1245. [[CrossRef](#)]
9. Humphreys, P.N.; West, J.M.; Metcalfe, R. *Microbial Effects on Repository Performance*; QRS-1378Q-1, Version 3.0; University of Huddersfield Repository: Didcot, UK, 2010.
10. Bassil, N.M.; Bewsher, A.D.; Thompson, O.R.; Lloyd, J.R. Microbial degradation of cellulosic material under intermediate-level waste simulated conditions. *Mineral. Mag.* **2015**, *79*, 1433–1441. [[CrossRef](#)]
11. Kyeremeh, I.A.; Charles, C.J.; Rout, S.P.; Laws, A.P.; Humphreys, P.N. Microbial community evolution is significantly impacted by the use of calcium isosaccharinic acid as an analogue for the products of alkaline cellulose degradation. *PLoS ONE* **2016**, *11*, e0165832. [[CrossRef](#)] [[PubMed](#)]
12. Kroll, A.; Behra, R.; Kaegi, R.; Sigg, L. Extracellular polymeric substances (EPS) of freshwater biofilms stabilize and modify CeO₂ and Ag nanoparticles. *PLoS ONE* **2014**, *9*, e110709. [[CrossRef](#)] [[PubMed](#)]
13. De Muynck, W.; Debrouwer, D.; De Belie, N.; Verstraete, W. Bacterial carbonate precipitation improves the durability of cementitious materials. *Cem. Concr. Res.* **2008**, *38*, 1005–1014. [[CrossRef](#)]
14. Charles, C.; Rout, S.; Garratt, E.; Patel, K.; Laws, A.; Humphreys, P. The enrichment of an alkaliphilic biofilm consortia capable of the anaerobic degradation of isosaccharinic acid from cellulosic materials incubated within an anthropogenic, hyperalkaline environment. *FEMS Microbiol. Ecol.* **2015**, *91*. [[CrossRef](#)] [[PubMed](#)]
15. Rout, S.P.; Charles, C.J.; Garratt, E.J.; Laws, A.P.; Gunn, J.; Humphreys, P.N. Evidence of the generation of isosaccharinic acids and their subsequent degradation by local microbial consortia within hyper-alkaline contaminated soils, with relevance to intermediate level radioactive waste disposal. *PLoS ONE* **2015**, *10*, e0119164. [[CrossRef](#)] [[PubMed](#)]
16. Charles, C.; Rout, S.; Patel, K.; Akbar, S.; Laws, A.; Jackson, B.; Boxall, S.; Humphreys, P. Floc formation reduces the pH stress experienced by microorganisms living in alkaline environments. *Appl. Environ. Microbiol.* **2017**, *83*, 02985–03016. [[CrossRef](#)] [[PubMed](#)]
17. Rout, S.P.; Radford, J.; Laws, A.P.; Sweeney, F.; Elmekawy, A.; Gillie, L.J.; Humphreys, P.N. Biodegradation of the alkaline cellulose degradation products generated during radioactive waste disposal. *PLoS ONE* **2014**, *9*, e107433. [[CrossRef](#)] [[PubMed](#)]
18. B.S.I. *Plastics—Determination of the Ultimate Anaerobic Biodegradation of Plastic Materials in an Aqueous System—Method by Measurement of Biogas Production*; BS ISO 14853:2005; British Standards Institute: London, UK, 2005.
19. Chang, C.-F.; Chen, J.-W. The experimental investigation of concrete carbonation depth. *Cem. Concr. Res.* **2006**, *36*, 1760–1767. [[CrossRef](#)]
20. Chen, M.-Y.; Lee, D.-J.; Tay, J.-H.; Show, K.-Y. Staining of extracellular polymeric substances and cells in bioaggregates. *Appl. Microbiol. Biotechnol.* **2007**, *75*, 467–474. [[CrossRef](#)] [[PubMed](#)]
21. Grant, W.D.; Holtom, G.J.; Kelly, N.O.; Malpass, J.; Rosevear, A.; Watkiss, P.; Widdowson, D. *Microbial Degradation of Cellulose Derived Complexants under Repository Conditions*; AEAT/ERRA-0301; AEA Technology: Didcot, UK, 2002.
22. Dunne, W.M. Bacterial adhesion: Seen any good biofilms lately? *Clin. Microbiol. Rev.* **2002**, *15*, 155–166. [[CrossRef](#)] [[PubMed](#)]
23. Zhu, T.; Dittrich, M. Carbonate precipitation through microbial activities in natural environment, and their potential in biotechnology: A review. *Front. Bioeng. Biotechnol.* **2016**, *4*, 4. [[CrossRef](#)] [[PubMed](#)]
24. Perry, T.D.T.; Klepac-Ceraj, V.; Zhang, X.V.; McNamara, C.J.; Polz, M.F.; Martin, S.T.; Berke, N.; Mitchell, R. Binding of harvested bacterial exopolymers to the surface of calcite. *Environ. Sci. Technol.* **2005**, *39*, 8770–8775. [[CrossRef](#)] [[PubMed](#)]
25. N.N.L. *Demonstration of Carbonation of the NRVB*; NNL(14)13296; National Nuclear Labs: Harwell, UK, 2015.
26. B.G.S. *Results of Laboratory Carbonation Experiments on NRVB Cement: Minerals and Waste Programme*; OR/14/048 Energy science programme; British Geological Survey: Keyworth, UK, 2014.

27. Almond, M.; Shaw, P.B.; Humphreys, P.N.; Chadha, M.J.; Niemela, K.; Laws, A.P. Behaviour of xyloisosaccharinic acid and xyloisosaccharino-1,4-lactone in aqueous solutions at varying pHs. *Carbohydr. Res.* **2012**, *363*, 51–57. [[CrossRef](#)] [[PubMed](#)]
28. Okshevsky, M.; Meyer, R.L. The role of extracellular DNA in the establishment, maintenance and perpetuation of bacterial biofilms. *Crit. Rev. Microbiol.* **2015**, *41*, 341–352. [[CrossRef](#)] [[PubMed](#)]
29. Das, T.; Sehar, S.; Manefield, M. The roles of extracellular DNA in the structural integrity of extracellular polymeric substance and bacterial biofilm development. *Environ. Microbiol. Rep.* **2013**, *5*, 778–786. [[CrossRef](#)] [[PubMed](#)]
30. Tang, L.; Schramm, A.; Neu, T.R.; Revsbech, N.P.; Meyer, R.L. Extracellular DNA in adhesion and biofilm formation of four environmental isolates: A quantitative study. *FEMS Microbiol. Ecol.* **2013**, *86*, 394–403. [[CrossRef](#)] [[PubMed](#)]
31. Watanabe, M.; Sasaki, K.; Nakashimada, Y.; Kakizono, T.; Noparatnaraporn, N.; Nishio, N. Growth and flocculation of a marine photosynthetic bacterium *Rhodovulum* sp. *Appl. Microbiol. Biotechnol.* **1998**, *50*, 682–691. [[CrossRef](#)]
32. Das, T.; Sehar, S.; Koop, L.; Wong, Y.K.; Ahmed, S.; Siddiqui, K.S.; Manefield, M. Influence of calcium in extracellular DNA mediated bacterial aggregation and biofilm formation. *PLoS ONE* **2014**, *9*, e91935. [[CrossRef](#)] [[PubMed](#)]
33. Brown, H.L.; Hanman, K.; Reuter, M.; Betts, R.P.; van Vliet, A.H.M. *Campylobacter jejuni* biofilms contain extracellular DNA and are sensitive to dnase i treatment. *Front Microbiol.* **2015**, *6*, 699. [[CrossRef](#)] [[PubMed](#)]



© 2017 by the authors. Licensee MDPI, Basel, Switzerland. This article is an open access article distributed under the terms and conditions of the Creative Commons Attribution (CC BY) license (<http://creativecommons.org/licenses/by/4.0/>).